High-pressure structural behavior of large-void CoSn-type intermetallics: Experiments and first-principles calculations

A. S. Mikhaylushkin,[1,2] Toyoto Sato,[3] Stefan Carlson,[4] Sergei I. Simak,[2] and Ulrich Häussermann[3]
[1]*Department of Physics, Uppsala University, P.O. Box 530, S-75121 Uppsala, Sweden*
[2]*Theory and Modeling, IFM, Linköping University, S-58183 Linköping, Sweden*
[3]*Department of Chemistry and Biochemistry, Arizona State University, P.O. Box 871604, Tempe, Arizona 85287-1604, USA*
[4]*Max-lab, Lund University, P.O. Box 118, SE-22100 Lund, Sweden*
(Received 29 June 2007; revised manuscript received 24 September 2007; published 8 January 2008)

The high-pressure structural behavior of the binary intermetallic compounds CoSn, FeSn, and NiIn with the peculiar void containing CoSn (B35)-type structure has been studied by means of room-temperature diamond anvil cell and high-temperature multianvil experiments, as well as by first-principles calculations. All three compounds remain structurally stable at pressures up to at least 25 GPa, whereas first-principles calculations predict high-pressure structural changes below 20 GPa. A plausible explanation for the discrepancy is that at room temperature, a sizable activation barrier inhibits kinetically the transformation into more close-packed polymorphs. It is supported by our experiments at temperatures around 1000 °C and a pressure of 10 GPa. At these conditions, NiIn transforms into the temperature-quenchable stoichiometric CsCl-type high-pressure phase, which has been predicted in our first-principles calculations. However, CoSn and FeSn decompose into a mixture of compounds richer and poorer in tin, respectively. Nevertheless, it might be possible that lower temperatures and higher pressures may afford theoretically predicted polymorphs. In particular, a phase transformation to the FeSi-type structure predicted for CoSn is of interest as materials with the FeSi-type structure are known for unusual thermal and transport properties.

DOI: 10.1103/PhysRevB.77.014102 PACS number(s): 64.70.K−, 62.50.−p, 71.20.Lp, 61.72.Qq

I. INTRODUCTION

The simple CoSn (B35) structure[1,2] violates the principle of high space filling and regular coordination of atoms, which is prevalent for structures of binary intermetallic compounds with the stoichiometry *AB*.[3] The characteristic feature of the CoSn structure is the presence of a void, or cage, defined by 20 atoms, and nonspherically coordinated Sn atoms. The space filling is just 55% for approximately equally sized atoms.[4] This is highly unusual for intermetallics, especially when considering the simplicity of the structure (six atoms per unit cell) and its stoichiometry (1:1). The CoSn structure occurs rarely among binary intermetallics. In addition to CoSn, there are other known representative FeSn, NiIn, PtTl, and RhPb.[5] The occurrence of a void containing binary intermetallic structure is puzzling, and the factors governing the structural stability of B35-type representatives are not completely understood. In the Pettifor structure map, which empirically orders *AB* compounds into domains of stable structures, the B35 compounds actually distribute in two fields, (CoSn, FeSn, RhPb) and (NiIn, PtTl), that are separated by domains of FeSi-type (B20) and CsCl-type (B2) compounds.[3] It appears that electron concentration should play a major role since B35-type representatives are confined to 12 or 13 valence electron compounds. Also, the radius ratio between transition metal (*A*) and main group element atoms (*B*) is important. When, for instance, Sn in B35-type FeSn and CoSn is exchanged for lighter (and smaller sized) Ge and Si, more close-packed structures become more stable. In particular, the monoclinic CoGe-type structure (for FeGe and CoGe) and the cubic FeSi-type structure (for FeSi and CoSi) emerge as ground states.

It is fundamental to materials physics to understand the stability of simple structure types in terms of compositional and pressure and/or temperature variations. In particular, compounds with the void containing CoSn structure are expected to collapse to higher density phases when exposed to external pressure. According to empirical structure maps and space filling arguments, FeSi- and CsCl-type polymorphs are likely candidates for high-pressure phases. Especially, in the B20 structure type each kind of atoms attains a homogeneous coordination by seven unlike neighbors and the space filling is increased to 64%.[4] As for the B35 structure, the B20 structure occurs predominantly for 12 and 13 electron systems. The possibility for the corresponding phase transformations is rather intriguing, considering that B20 representatives often display interesting magnetic, thermal, and transport properties.[6–8] Therefore, high-pressure phases of FeSn and CoSn with the B20 structure would increase the number of 12 and 13 electron compounds, with the properties potentially interesting for applications. So far, quenchable FeSi-type high-pressure phases have been known for MnGe, CoGe, and RhGe.[9,10] We noticed that our previous theoretical studies of the CoSn system, indeed, predicted the FeSi-type structure as a high-pressure phase above 26 GPa.[11] However, so far, no phase transformation has been observed experimentally.[2]

The present combined experimental and theoretical study is devoted to the structural behavior of the large-void CoSn-type intermetallics CoSn, FeSn, and NiIn at high pressure and/or temperature, and attempts to obtain other 12 and 13 electron materials. We have conducted diamond anvil cell (DAC) and multianvil experiments for CoSn, FeSn, and NiIn at room temperature and high temperature, respectively, as well as first-principles electronic structure calculations described in detail in the following sections.

II. EXPERIMENTAL AND COMPUTATIONAL DETAILS

A. Sample preparation and analysis

Crystalline samples of the CoSn and FeSn were prepared from reaction mixtures of the pure elements with a molar $A=(\mathrm{Co,Fe}):\mathrm{Sn}$ ratio of 1:3, thus employing Sn as both reactant and flux medium. The mixtures (0.5 g) were pressed into pellets prior to loading into quartz ampoules, which were sealed under vacuum. Subsequently, the ampoules were heated to 650 °C, held at this temperature for 24 h, and finally quenched in water. Excess Sn was dissolved with 4*M* HCl over a period of two days, and the crystalline remains were washed with de-ionized water. The flux technique is not applicable for preparing NiIn because of the presence of an In richer phase (Ni_2In_3) with a peritectic decomposition temperature almost identical to NiIn. Therefore, NiIn was synthesized by arc melting stoichiometric amounts of Ni and In, and subsequent annealing at 700 °C for 72 h. The resulting product contained a small amount of Ni_2In_3, which could be removed by leaching the sample in 4*M* HCl. The acid attacked Ni_2In_3 at a much faster rate than NiIn.

CoSn, FeSn, and NiIn were characterized by x-ray powder diffraction (Guinier camera Cu $K\alpha$; Si standard). All the lines of the powder patterns could be indexed with a hexagonal cell (program TREOR97).[12] Lattice parameters were obtained from least-square refinements of the measured and indexed lines (program PIRUM).[13] The composition of the compounds was analyzed by electron microprobe techniques to check for possible homogeneity ranges (JEOL JXA-8600, operated at 15.0 kV and 10.0 nA). Co, Fe, Ni (*K*), Sn, and In (*L*) elemental metals were used as standards. The ZAF [atomic number (Z), absorption (A), and fluorescence (F)] correction procedure was employed for quantitative composition determination.

For thermal stability studies, differential scanning calorimetry (DSC, TA instrument DSC 2920) was employed. Samples were enclosed in Al pans. Calibration of the instrument was performed with indium, lead, tin, and zinc as standards. Empty aluminum pans were used for baseline correction. Experiments were done under a flow of He gas (30 ml/min) and with a temperature increase rate of 10 K/min.

B. High-pressure investigations

For DAC experiments, powdered samples of CoSn, FeSn, and NiIn were loaded with Ar pressure-transmitting medium and a small ruby crystal (1–2 μm diameter spheres) in a membrane driven DAC.[14] A preindented stainless-steel gasket with a hole of 125 μm diameter and 30 μm thickness was used. For pressure determination, the ruby fluorescence technique[15] and the calibration scale by Mao *et al.* were applied.[16] The diffraction experiments were carried out at room temperature at the high-pressure dedicated beamline ID30, European Synchrotron Radiation Facility (ESFR), Grenoble, France. X rays were monochromatized to $\lambda=0.3738(1)$ Å and the beam was focused to a 0.02×0.03 mm^2 spot size at the sample position. Reflections with $2\theta<23°$ could be collected, and the pressure cell was oscillated ±3° perpendicular to the x-ray beam in order to increase the powder averaging. The powder diffraction rings were collected with an online imaging plate detector.[17] A diffraction pattern of Si was used to determine the sample to detector distance (310.042 mm). Corrections for spatial distortion, calculation of imaging plate pixel size (0.07×0.08 mm^2), and subsequent integration over the complete powder rings were performed using the software FIT2D.[18] Unit cell parameters were obtained by indexing and least-square refinement with the program DICVOL91.[19] Equations of state were described by the Birch-Murnaghan equation using the software EOSFIT.[20]

For multianvil experiments, powdered samples of FeSn, CoSn, and NiIn were pressed into pellets, which were placed in boron nitride (BN) capsules. Subsequently, the BN capsule was positioned with a graphite furnace and a zirconia insulating sleeve in a magnesia octahedron with 14 mm edge length (see Ref. 21 for details). Samples were pressurized to 10 GPa by a 6–8 multianvil high-pressure device, with tungsten carbide cubes truncated to 8 mm edge length. After reaching the target pressure, the samples were heated to 1000 °C and quenched after 1 h.

C. First-principles calculations

Total energy calculations were performed in the framework of the frozen core all-electron projector augmented wave method,[22] as implemented in the Vienna *ab initio* simulation package (VASP).[23] This computational method has shown outstanding efficiency and reliability for the calculation of various physical properties and structural transformations of simple and complex materials.[24] All considered compounds were calculated the same way. The energy cutoff was set to 400 eV. Exchange and correlation effects were treated by the generalized gradient approximation.[25] The integration over the Brillouin zone was done on a grid of special *k* points determined according to the Monkhorst-Pack scheme.[26] We used *k* point grids, which were converged with respect to the total energy for each structure. For the structural relaxation and force calculations, the integration was carried out according to the Methfessel-Paxton scheme,[27] while accurate total energy calculations were done with the modified tetrahedron method with Blöchl correction.[28] All necessary convergence tests were performed and total energies were converged to within 1.0 meV/atom. The enthalpies and equations of state were extracted by accurate numerical interpolations of total energy vs volume curves with the Birch-Murnaghan equation.[29] For interpolation, 20–30 points were used for each curve, which yields a regular interpolation error of 0.5–1.0 meV/atom.

III. RESULTS

A. Ground state properties of the CoSn, FeSn, and NiIn compounds

At ambient conditions, CoSn, FeSn, and NiIn crystallize in the hexagonal CoSn-type (B35) structure (space group $P6/mmm$).[1,2] This structure contains six atoms in the unit cell, which are distributed over three special positions: Co 3*f*

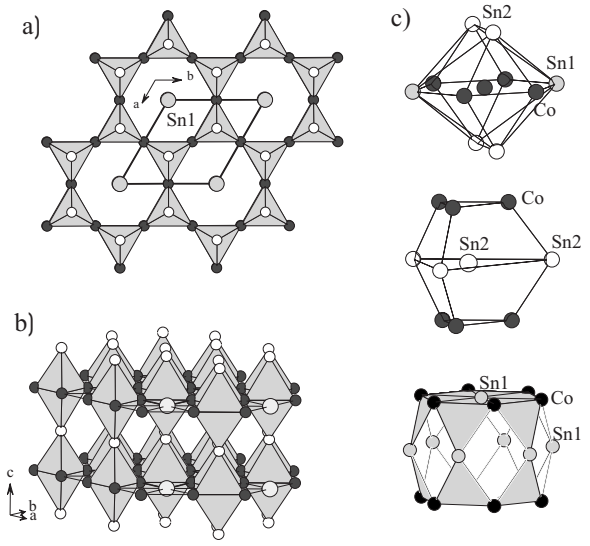

FIG. 1. The crystal structure of CoSn (B35). (a) View along [001]. (b) Approximate view along [110] indicating the location of the void. (c) Coordination polyhedra around Co, Sn2, and the void. Co, Sn1, and Sn2 atoms are displayed as black, gray, and white circles, respectively.

$(1/2,0,0)$, Sn1 1*a* (0,0,0), and Sn2 2*d* $(1/3,2/3,1/2)$. The CoSn-type structure can be divided into two different kinds of planar nets which are stacked alternately along the *c* axis (Fig. 1). One net contains all of the Co atoms and one sort of Sn atoms (Sn1) in a ratio 3:1, and corresponds to a close-packed layer. The second net represents a honeycomb net consisting exclusively of the other sort of Sn atoms (Sn2). These Sn2 atoms are situated above and below the centers of Co_3 triangles in the close-packed layer, which yields a framework of corner condensed trigonal bipyramids. The fact that the density of the honeycomb layer is just half of the close-packed layer introduces a void in the CoSn structure, which is centered at 1*b* $(0,0,1/2)$. Additionally, the Sn1 atoms obtain an unusual hexagonal planar coordination of six Co atoms. On the other hand, the coordination polyhedra of Sn2 and Co are rather spherical, consisting of nine and ten atoms, respectively.

The refined lattice parameters and microprobe compositions of the three compounds are compiled in Table I. The unit cell volume and c/a ratio increase slightly from CoSn to NiIn to FeSn. The lattice parameters are in very good agreement with earlier reported values.[1,2,30,31] Our compositional analysis confirms the 1:1 stoichiometry of all three compounds. In the binary alloy phase diagrams assembled by Massalski, the FeSn and CoSn compounds are reported as "line" phases, whereas NiIn has a small homogeneity range.[32] In a later investigation of the Ni-In system, however, NiIn was found to be a stoichiometric compound.[31] To settle still present doubts into the CoSn-type structure of the NiIn compound, we performed electron diffraction studies which showed the absence of diffuse scattering or superstructure reflections in NiIn and further confirmed the space group symmetry $P6/mmm$.[33] Results of our first-principles calculations of the structural parameters for the ground state volume, presented in Table II, agree well with the experimental data.

TABLE I. Experimental lattice parameters and compositions for FeSn, CoSn, and NiIn.

	FeSn	CoSn	NiIn
a (Å)	5.2970(3)	5.2794(3)	5.2436(6)
c (Å)	4.4494(5)	4.2598(3)	4.3505(7)
c/*a*	0.840	0.807	0.830
V (Å^3/cell)	108.12	102.82	103.6
Composition (at. %)	49.6(3) Fe	49.4(2) Co	49.4(4) Ni
	50.4(3) Sn	50.6(2) Sn	50.6(4) In

Concerning the magnetic properties of these intermetallics, FeSn is reported to be antiferromagetic (AFM) with a Néel temperature of 365 K, whereas CoSn and NiIn are paramagnetic (PM).[30,34,35]

B. Diamond anvil cell experiments and theoretical predictions

The high-pressure structural behavior of the FeSn, CoSn, and NiIn was studied at room temperature using a DAC. Both experimental and theoretical results are shown in Fig. 2. For the CoSn, a pressure of up to 38 GPa was applied. This pressure exceeds the maximum pressure applied in a previous DAC study (26 GPa),[2] and is above the pressure for theoretically predicted phase transitions to the FeSi-type and CsCl-type structures at 26 and 36 GPa,[11] respectively. The FeSn and NiIn were investigated up to 28 GPa. For the FeSn, this corresponds approximately to the pressure applied in a

TABLE II. Calculated lattice parameters and bulk moduli for FeSn, CoSn, and NiIn.

	FeSn-NM	FeSn-FM	FeSn-AFM	CoSn	NiIn
E (meV/f.u.)					
a (Å)	5.296	5.295	5.283	5.302	5.287
c (Å)	4.290	4.448	4.454	4.226	4.383
c/*a*	0.810	0.840	0.843	0.797	0.829
V (Å^3/cell)	104.2	108	107.6	102.9	106.1
B_0 (GPa)	130	98	101	127	102
$B_{0\mathrm{exp}}$ (GPa)			95(2)	115(4)	153(3)
$B'_{0\mathrm{exp}}$ (GPa)			6.3(4)	5.8(5)	4 (fixed)

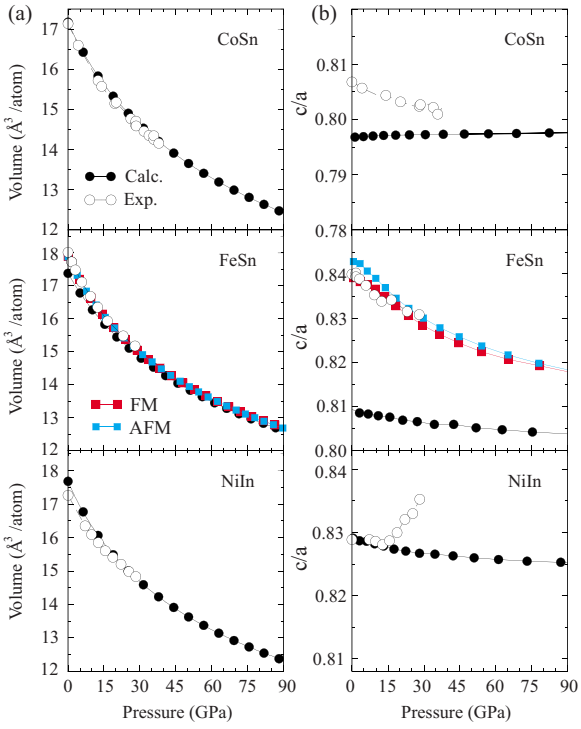

FIG. 2. (Color online) (a) Equation of state and (b) c/a variation of CoSn, FeSn, and NiIn according to DAC experiments and theory.

recent study of the equation of states of several Fe-Sn intermetallics.[36] The NiIn has not been so far a subject of high-pressure studies.

For all three compounds, no structural change is observed in the investigated pressure ranges [Fig. 2(a)]. Interestingly, the c/a ratio remains almost unchanged with pressure. This holds especially for the calculated ratios [Fig. 2(b)]. Therefore, the increase of the c/a ratio for the NiIn compound above 15 GPa may indicate the onset of a pressure induced structural instability. The V-P relations were fit to the third-order Birch-Murnaghan equation. The extracted bulk moduli for the CoSn and FeSn compounds, 115(4) and 95(2) GPa, respectively, are slightly higher and lower compared to earlier investigations [127(8) Gpa Ref. 2 and 86(2) GPa Ref. 36], respectively. The NiIn has the highest bulk modulus among the three compounds [153(3) GPa]. The equations of state for the three CoSn-type compounds obtained from first-principles calculations are in very good agreement with experimental data [cf. Fig. 2(a)]. The values of the calculated and experimental bulk moduli also demonstrate good agreement (Table II), apart for NiIn where the theoretical bulk modulus is considerably lower than the experimental one. This discrepancy is most likely related to the experimentally observed c/a increase above 15 GPa. We note that it was not possible to extract a derivative from the experimental P-V data. The effect of magnetism on structural properties of the FeSn compound manifests itself in a slightly enlarged equilibrium volume and c/a ratio. The structural parameters for the ferromagnetic and antiferromagnetic solutions are very similar.

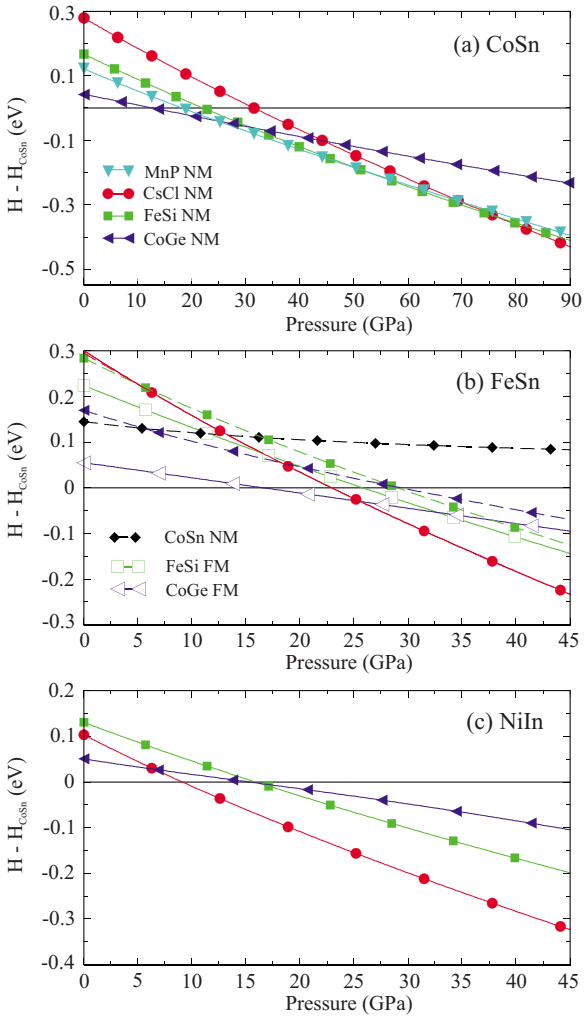

FIG. 3. (Color online) Enthalpy as a function of pressure for (a) CoSn, (b) NiIn, and (c) FeSn. The structure most stable at a certain pressure has the lowest value. The enthalpy of the CoSn-type structure is taken as reference.

To investigate the pressure stability of the CoSn-type structure for the FeSn, CoSn, and NiIn compounds, we calculated enthalpies for the three systems and considered the structure types FeSi (B20), CsCl (B2), NiAs (B8$_1$), orthorhombic MnP, and monoclinic CoGe as possible alternatives. This selection is based on Pettifor's empirical structure map for AB compounds.[3] The enthalpies of the most competitive structures as a function of pressure are shown in Fig. 3. The CoSn transforms at 13 GPa from the hexagonal CoSn-type structure to the monoclinic CoGe at 25 GPa to the orthorhombic MnP-type structure. At further compression, the FeSi-type and CsCl-type structures become stable above 52 and 75 GPa, respectively [Fig. 3(a)]. Note that a full relaxation of structural parameters performed in the present work modifies the results of our previous study,[11] where the transitions CoSn type→FeSi type and FeSi type→CsCl type above 26 and 36 GPa, respectively, were predicted. The compound FeSn is an antiferromagnet with a magnetic moment of $\sim 1.8\mu_B$ on the Fe atoms. The Sn1-type atoms attain

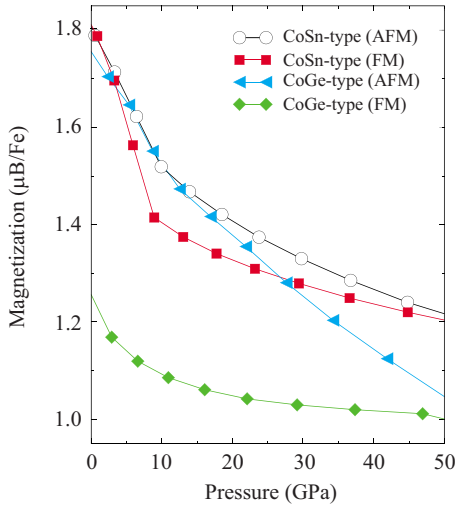

FIG. 4. (Color online) Magnetic moment of FeSn in the CoSn- and CoGe-structures type as a function of pressure.

a small magnetic moment of about $0.1\mu_B$ and are magnetized with AFM ordering parallel to the spin of the Fe atoms, which are situated in the same layer. The ferromagnetic (FM) solution is energetically only slightly less favorable and almost degenerate with the AFM solution [and therefore not shown in Fig. 3(b)]. The magnetic moment of the Fe atoms for both AFM and FM CoSn-type FeSn reduces slightly with pressure (Fig. 4). FeSn transforms from the AFM CoSn type first into the FM CoGe-type structure at 17 GPa and then into the NM CsCl-type structure above 27 GPa. If only the nonmagnetic solutions are considered, the CoSn type $\rightarrow$CoGe type and CoGe type$\rightarrow$CsCl type phase transitions will occur at considerably lower pressures. The NiIn [Fig. 3(c)] transforms directly from the CoSn-type structure into the CsCl-type structure at 9 GPa. For all three considered compounds, the CsCl-type structure remains stable up to the highest considered pressure of 90 GPa. The CsCl-type structure, where each atom is coordinated by eight unlike atoms, is the end member of each sequence.

To summarize, theory predicts for all three CoSn-type systems high-pressure structural transitions in a pressure range which has been accessed by the DAC experiments. For instance, for CoSn at 40 GPa, the FeSi-type structure is about 120 meV/atom ($\sim$1385 K) more favorable than the CoSn-type structure. For FeSn and NiIn at 30 GPa, the energy difference between the CoSn and CsCl structures are about 80 meV/atom ($\sim$925 K) and 200 meV/atom ($\sim$2310 K), respectively. The discrepancy between our room-temperature experiments and theoretical calculations is due to a sizable activation barrier, which kinetically inhibits the direct transition of compounds with the CoSn structure into more close-packed polymorphs. A similar situation has been reported for the FeSi type$\rightarrow$CsCl type high-pressure transformation of FeSi and RuSi.[37–39] To evaluate further the stability of CoSn-type FeSn, CoSn, and NiIn, we performed multianvil high-pressure high-temperature experiments.

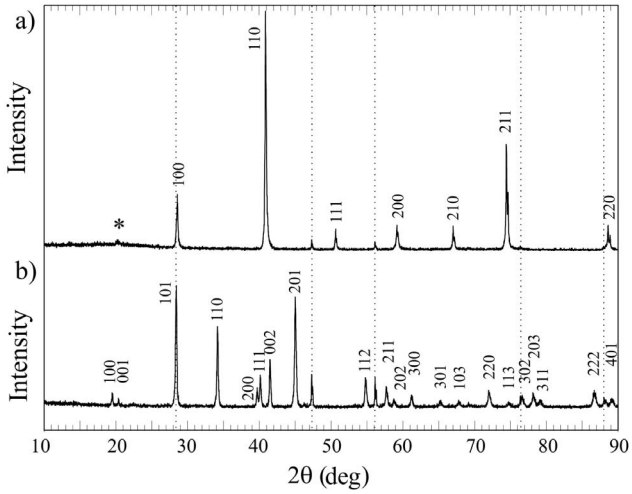

FIG. 5. (a) X-ray powder diffraction pattern of the CsCl-type high-pressure phase of NiIn. (b) X-ray powder diffraction pattern of NiIn obtained after reversion to the CoSn-type phase. The broken vertical lines mark the location of the reflections from the Si standard. The asterisk indicates a possible reflection from the high-pressure phase of NiIn which, however, cannot be described with the CsCl structure.

C. Multianvil high-temperature experiments

Samples of the FeSn, CoSn, and NiIn compounds were subjected to 10 GPa and temperatures around 1000 °C in multianvil experiments and subsequently quenched. The compounds FeSn and CoSn decomposed into a mixture of phases $FeSn_2/Fe_3Sn_2$ and $CoSn_2/Co_3Sn_2$, respectively, while the NiIn sample yielded quantitatively a high-pressure phase. The x-ray powder diffraction pattern of this phase corresponded to that of the primitive cubic CsCl-type structure. The lattice parameter was refined as $a=3.1197(2)$ Å [Fig. 5(a) and Table III]. Microprobe analysis confirmed that the 1:1 stoichiometric composition of CoSn-type NiIn was maintained in its high-pressure CsCl-type phase. The experimental lattice parameter corresponds well to the theoretical equilibrium lattice parameter of the CsCl-type NiIn phase.

The thermal stability of the high-pressure NiIn phase was studied up to 550 °C by DSC (Fig. 6). A small endothermic feature at around 250 °C is followed by an exothermic reaction at around 310 °C. The sample was investigated by x-ray powder diffraction after the DSC study, and the diffraction pattern showed a quantitatively restituted CoSn-type phase [$a=5.241(1)$ Å and $c=4.350(2)$ Å], which is shown in Fig. 5(b). The small endothermic feature corresponds possibly to

TABLE III. Lattice parameter, composition, and bulk modulus for CsCl-type NiIn.

	Experimental	Calculated
a (Å)	3.120(2)	3.158
B_0 (GPa)		121
Composition (at. %)	49.8(3) Ni	
	50.2(3) In	

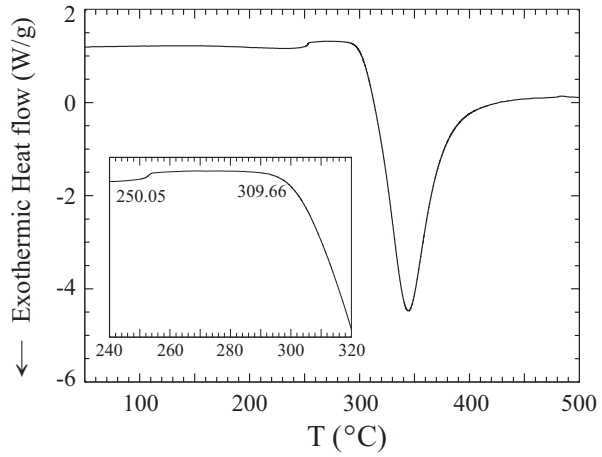

FIG. 6. DSC trace for the CsCl-type high-pressure phase of NiIn. The inset represents a blowup of the temperature region before the phase transition.

an order-disorder transition in CsCl-type NiIn phase, as observed in similar systems,[40] whereas the much larger thermal effect has to represent the reverse transition into the CoSn-type phase. In the older literature, CsCl-type NiIn has been discussed as a (nonstoichiometric) high-temperature form of NiIn.[41] However, our study shows clearly that the high-pressure CsCl-type phase of NiIn obtained in our experiments is stoichiometric. The equilibrium volume of CsCl-type NiIn is about 12% smaller than that of the CoSn-type ground state, which agrees well with the theoretical prediction (cf. Table III).

The multianvil experiments demonstrate that large-void CoSn-type intermetallics lift their surprising high pressure stability observed with DAC experiments when pressure and high temperatures are applied at the same time. Thus, the phase transitions predicted by theory appear to be kinetically hindered. For NiIn, the CsCl-type phase, which theory predicts to be stable above 9 GPa, can be quenched to ambient pressure. The CoSn and FeSn compounds undergo a phase separation at the conditions where the NiIn high-pressure phase was obtained. However, the application of lower temperatures and higher pressures may yield stoichiometric high-pressure phases for these systems as well.

IV. DISCUSSION

Theoretical calculations predict that the three CoSn-type systems FeSn, CoSn, and NiIn display different sequences of high-pressure structural transitions: For CoSn, we find CoSn type → CoGe type → MnP type → FeSi type → CsCl type; for FeSn, CoSn type → CoGe type → CsCl type; and for NiIn, CoSn type → CsCl type. The CsCl-type structure, where each atom is coordinated by eight unlike atoms, is the end member of each sequence. This is expected for *dp* bonded intermetallic *AB* compounds from space filling arguments.[11] Interestingly, the FeSi-type structure with potential interesting properties for 12 and 13 electron compounds occurs only in the sequence for CoSn.

The FeSi B20 structure with homogeneously coordinated atoms forms especially for silicides and to a minor extent for germanides.[5] Applying high-pressure synthesis conditions increases the number of germanide representatives considerably.[10,11] With Sn (and In), an appreciable size difference between transition metal *A* (smaller) and main group element *B* (larger) is introduced. The ambient pressure large-void CoSn structure for compounds *AB* appears as a consequence of such a "size mismatch." This size mismatch gives rise to a quasisegregation of *A* and *B* into graphitic nets with a composition B_2 and close-packed nets with a composition A_3B. Associated with this separation is an irregular coordination of atoms [cf. Figs. 1(b)–1(d)].

The bonding situation in CoSn-type compounds has been interpreted with a covalent bonded B_2 substructure embedded into a metallic bonded environment of A_3B layers.[11] With pressure, the "size mismatch" between *A* and *B* diminishes and more close-packed structures with a more homogeneous coordination of atoms are realized. However, the structural rigidity of the FeSi type, which only allows a displacement of atoms along the body diagonals of the cubic unit cell, limits its occurrence as intermediate phase in the high-pressure structural sequence of CoSn-type materials. More flexible structures, such as the monoclinic CoGe type, turn out to be more favorable. Ultimately, the kind of intermediate structures on the way to the CsCl-type end member will depend on the electronic structure of the particular system.[42]

The theoretically predicted sequences of high-pressure structural transitions for FeSn, CoSn, and NiIn have not been observed in room-temperature DAC experiments. This discrepancy is ascribed to an energy barrier inhibiting kinetically these phase transformations. At temperatures around 1000 °C and a pressure of 10 GPa, CoSn-type NiIn transforms into the CsCl high-pressure phase, which is quenchable, whereas CoSn and FeSn decompose at these conditions. Importantly, the fact that the CsCl-type high-pressure phase of NiIn can be recovered at ambient conditions strongly supports the idea of kinetically hindered phase transitions for CoSn-type materials. CsCl-type NiIn reverts to the CoSn-type ground state when heating to about 310 °C.

V. SUMMARY

The high-pressure structural behavior of the large-void CoSn-type intermetallics FeSn, CoSn, and NiIn has been examined both experimentally and by first-principles calculations. The experiments included room-temperature DAC and high-temperature multianvil studies. Theory predicted high-pressure structural transitions for all materials which, however, are kinetically hindered and could not be observed in the DAC experiments. High temperature multianvil experiments afforded a CsCl-type high-pressure phase for NiIn. This phase is in accord with the theoretical prediction. Instead of decomposing, CoSn and FeSn may also transform to theoretically predicted polymorphs if lower temperatures

and/or higher pressures are applied in multianvil experiments.

ACKNOWLEDGMENTS

This work was supported by the Swedish Research Council (VR), the Swedish Foundation for Strategic Research (SSF), and the Carl Trygger foundation for scientific research (CTS). We further acknowledge the Swedish National Infrastructure for Computing (SNIC) program for computational resource support. We are grateful to Michael Hanfland, ESRF, for assistance in the high-pressure DAC experiments.

[1] O. Nial, Z. Anorg. Allg. Chem. **238**, 287 (1938).
[2] A. K. Larsson, M. Haeberlein, S. Lidin, and U. Schwarz, J. Alloys Compd. **240**, 79 (1996).
[3] D. G. Pettifor, *Bonding and Structure of Molecules and Solids* (Clarendon, Oxford, 1995).
[4] E. Parth'e, Z. Kristallogr. **115**, 52 (1961).
[5] *Pearson's Handbook of Crystallographic Data for Intermetallic Phases*, 2nd ed., edited by P. Villars and L. D. Calvert (ASM International, Materials Park, OH, 1991); *ibid.*, Desk ed. (ASM International, Materials Park, OH, 1997).
[6] M. Bat'kova, I. Bat'ko, and M. Mihalik, Solid State Commun. **141**, 412 (2007); N. Manyala, Y. Sidis, J. F. Ditusa, G. Aeppli, D. P. Young, and Z. Fisk, Nat. Mater. **3**, 255 (2004); S. Paschen, E. Felder, M. A. Chernikov, L. Degiorgi, H. Schwer, H. R. Ott, D. P. Young, J. L. Sarrao, and Z. Fisk, Phys. Rev. B **56**, 12916 (1997); C. Fu, M. P. C. M. Krijn, and S. Doniach, *ibid.* **49**, 2219 (1994); Z. J. Pan, L. T. Zhang, and J. S. Wu, J. Appl. Phys. **101**, 033715 (2007); Y. K. Kuo, K. M. Sivakumar, S. J. Huang, and C. S. Lue, *ibid.* **98**, 123510 (2005).
[7] L. F. Mattheiss and D. R. Hamann, Phys. Rev. B **47**, 13114 (1993).
[8] T. Jarlborg, Phys. Rev. B **51**, 11106 (1995); **59**, 15002 (1999); Phys. Lett. A **236**, 143 (1997).
[9] V. I. Larchev and S. V. Popova, J. Less-Common Met. **87**, 53 (1982).
[10] H. Takizawa, T. Sato, T. Endo, and M. Shimada, J. Solid State Chem. **73**, 40 (1988).
[11] S. I. Simak, U. Häussermann, I. A. Abrikosov, O. Eriksson, J. M. Wills, S. Lidin, and B. Johansson, Phys. Rev. Lett. **79**, 1333 (1997).
[12] P.-E. Werner, L. Eriksson, and M. Westdahl, J. Appl. Crystallogr. **18**, 367 (1985).
[13] P.-E. Werner, Ark. Kemi **31**, 513 (1969).
[14] R. Letoullec, J. P. Pinceaux, and P. Loubeyre, High Press. Res. **1**, 77 (1988).
[15] G. J. Piermarini, S. Block, J. D. Barnett, and R. A. Forman, J. Appl. Phys. **46**, 2774 (1975).
[16] H. K. Mao, J. Xu, and P. M. Bell, J. Geophys. Res., [Solid Earth Planets] **91**, 4673 (1986).
[17] M. Thoms, S. Bachau, D. Häusermann, M. Kunz, T. Le Bihan, M. Mezouar, and D. Strawbridge, Nucl. Instrum. Methods Phys. Res. A **413**, 175 (1998).
[18] A. Hammersley, *FIT2D V10.3 Reference Manual V4.0* (ESFR, Grenoble, 1998).
[19] A. Boultif and D. Loüer, J. Appl. Crystallogr. **24**, 987 (1991).
[20] R. J. Angel, in *High-pressure, High-temperature Crystal Chemistry*, edited by R. M. Hazen and R. T. Downs, Reviews in Mineralogy and Geochemistry Vol. 41 (Mineralogical Society of America, Washington, DC, 2001).
[21] K. Leinenweber and J. Parise, J. Solid State Chem. **114**, 277 (1995).
[22] P. E. Blöchl, Phys. Rev. B **50**, 17953 (1994); G. Kresse and D. Joubert, *ibid.* **59**, 1758 (1999).
[23] G. Kresse and J. Hafner, Phys. Rev. B **48**, 13115 (1993); G. Kresse and J. Furthmüller, Comput. Mater. Sci. **6**, 15 (1996).
[24] B. Grabowski, T. Hickel, and J. Neugebauer, Phys. Rev. B **76**, 024309 (2007); S. Mehta, J. D. Price, and D. Alfe, J. Chem. Phys. **125**, 194507 (2006); P. Souvatzis, O. Eriksson, and M. I. Katsnelson, Phys. Rev. Lett. **99**, 015901 (2007); A. S. Mikhaylushkin, U. Häussermann, B. Johansson, and S. I. Simak, *ibid.* **92**, 195501 (2004); A. S. Mikhaylushkin, S. I. Simak, B. Johansson, and U. Häussermann, J. Phys. Chem. Solids **67**, 2132 (2006); U. Häussermann, Chem.-Eur. J. **9**, 1471 (2002); A. S. Mikhaylushkin, S. I. Simak, B. Johansson, and U. Häussermann, Phys. Rev. B **76**, 092103 (2007); U. Häussermann, O. Degtyareva, A. S. Mikhaylushkin, K. Soderberg, S. I. Simak, M. I. McMahon, R. J. Nelmes, and R. Norrestam, *ibid.* **69**, 134203 (2004); A. S. Mikhaylushkin, S. I. Simak, B. Johansson, and U. Häussermann, *ibid.* **72**, 134202 (2005); A. S. Mikhaylushkin, J. Nylen, and U. Häussermann, Chem.-Eur. J. **11**, 4912 (2005).
[25] Y. Wang and J. P. Perdew, Phys. Rev. B **44**, 13298 (1991); J. P. Perdew, J. A. Chevary, S. H. Vosko, K. A. Jackson, M. R. Pederson, D. J. Singh, and C. Fiolhais, *ibid.* **46**, 6671 (1992).
[26] H. J. Monkhorst and J. D. Pack, Phys. Rev. B **13**, 5188 (1976).
[27] M. Methfessel and A. T. Paxton, Phys. Rev. B **40**, 3616 (1989).
[28] P. E. Blöchl, O. Jepsen, and O. K. Andersen, Phys. Rev. B **49**, 16223 (1994).
[29] F. D. Murnaghan, *Finite Deformation of an Elastic Solid* (Wiley, New York, 1951); F. Birch, J. Appl. Phys. **9**, 279 (1938); Phys. Rev. **71**, 809 (1947); J. Phys. Chem. Solids **38**, 175 (1977); J. Geophys. Res. **83**, 1257 (1978).
[30] C. Djega-Mariadassou, P. Lecocq, and A. Michel, Ann. Chim. (Rome) **59**, 175 (1969).
[31] P. Durussel, G. Burri, and P. Feschotte, J. Alloys Compd. **257**, 253 (1997).
[32] *Binary Alloys Phase Diagrams*, 2nd ed., edited by T. B. Massalski (ASM International, Materials Park, OH, 1996).
[33] T. Yokosava and U. Häussermann (unpublished).
[34] M. Larsson, S. Byström, K. Marklund, and T. Lundquist, Phys. Scr. **9**, 51 (1974).
[35] L. Häggström, T. Ericson, and R. Wäppling, Phys. Scr. **11**, 94 (1975).
[36] H. Giefers and M. Nicol, J. Alloys Compd. **422**, 132 (2006).
[37] L. Vocadlo, G. D. Price, and I. G. Wood, Acta Crystallogr., Sect. B: Struct. Sci. **55**, 484 (1999).
[38] L. Vocadlo, G. D. Price, and I. G. Wood, Acta Crystallogr., Sect. B: Struct. Sci. **56**, 369 (2000).
[39] D. P. Dobson, L. Vocadlo, and I. G. Wood, Am. Mineral. **87**, 784

(2002).
[40] H. V. Keer, *Principles of the Solid State* (New Age Publishers, New Delhi, India, 1993); T. Suzuki and M. Hagiwara, Metall. Trans. A **6A**, 241 (1975); P. Tissot and R. Dallenbach, Thermochim. Acta **25**, 143 (1978).
[41] E. Hellner and F. Laves, Z. Naturforsch. **2A**, 177 (1947).
[42] R. Demchyna, S. Leoni, H. Rosner, and U. Schwarz, Z. Kristallogr. **221**, 420 (2006).